

# Photovoltaic Solar Water Pumping by Predictive Control of Induction Motor

Zakaria Lammouchi<sup>1\*</sup>, Abderrahim Allal<sup>1</sup>

<sup>1</sup>Faculty of Technology, University of El Oued, 39000 El Oued, P.O.B. 789, Algeria

Corresponding author, e-mail: lammouchi-zakaria@univ-eloued.dz

Received 03/08/ 2023, Accepted 08/01/ 2024

## Abstract

The advantages of using the photovoltaic system for water pumping are easy assembly and installation of components, low maintenance and noise-free operation. This paper deals with the design and control of photovoltaic (PV) system interconnected with a three-phase voltage source inverter (VSI) and a motor-pump assembly. This work also focuses on demonstrating the efficiency and performance of Predictive control (FS-MPC). An incremental conductance (InC) modified with the flow-rate power control is proposed to exploit maximum power from a PV array, which is eligible to regulate the flow rate corresponding to desired flow, high gain observer (HGO) has been utilized to estimate the mechanical and magnetic states, which uses only the measured stator currents and control voltage. Results of simulation studies demonstrate that robustness and efficiency of the system are maintained under any insolation level.

**Keywords:** Water Pump, Photovoltaic (PV), incremental conductance (InC), Induction Motor Drive (IMD), Finite-States Model Predictive Control (FS-MPC), cost function,.

**Tob Regul Sci.**™ 2024;10(1):207-223

**DOI:** [doi.org/10.18001/TRS.10.1.15](https://doi.org/10.18001/TRS.10.1.15)

## Introduction

The impact and continuous consumption of energy is the primary cause of all environment disaster. Today's, renewable energy is the best solution of replacement this energy, photovoltaic (PV) power generation is the better technology that directly generates electrical power [1]. The irrigation sector is pioneer in solar PV powers where this energy is largely used for water pumping [2].

The advantages of employing PV power for water pumps, ease of elements assembly and installation, lower maintenance, noise free operation (no moving parts), Generally, the elements of Single-Stage PV with water pumping system consists of three parts: solar PV array, inverter converter and group of motor - pump [2]. DC motor was the first motor has ben using for Solar PV water pumping. However, with virtues related with the induction motor, it has replaced DC motors [3].

Maximum power extraction techniques have occupied a part in scientific research. Therefore, different techniques have been developed in order to work at the Maximum Power Point (MPP), which differ in its complexity, speed and precision when tracing this point [1]. Few of publications, developed and improved incremental conductance algorithms as per consumers' requirement. Here, InC based MPPT algorithm with a derating mechanism is applied, which is eligible of operating even under fixed duty ratio to regulate the flow rate corresponding to desired flow [2-4].

As we know that there are several topologies available for solar water pumping . With double stage topology of solar PV array system, boost converter is used for tracking of maximum power point , which is vastly in use for MPPT [5].

While, for single stage topology of same system, only one converter (inverter) is utilized in place of first converter , which is used to achieve both the control of DC link voltage and MPPT [6].

Different control strategies have been proposed over the last years to control power converters. Among them ,field-oriented control (FOC) method and direct torque control (DTC) method [7]. These control strategies have some unsatisfactory characteristics. Finite-States Model Predictive Control (FS-MPC) appears as an attractive alternative and offers a completely different and powerful approach [12], many papers have studied it recently due to its fast dynamic response, no need for linear controllers, extremely simple, very good performance [9].

For FS-MPC control, the principle is to chosen the best switching vector that can minimize the cost function [9], this function should be summarizes the desired behavior of the system by minimizing the tracking error between reference and predicted variables[10].

Generally, in the process of selecting optimal voltage vector, all feasible vectors need to be considered, eight switching states for two-level inverter in ours system [11][12].

Eradicating the use of speed sensors on the induction motor shaft represents both a financial saving and an increased reliability [15], in the past years, Several efforts have focused to control of the IM drive without mechanical sensor [8-20]. In this framework, we have proposed an interconnection observer of Induction Motor Drive for Water Pumping to estimate the IM speed, load torque and rotor flux through only stator voltage and current values .The idea is to design an observer for the whole system by interconnected between two subsystems extract from the all motor -pump model [16].

Therefore, this paper deals with following aspects:

Single stage PV array design without DC-DC converter with only one VSI .

Reference Speed calculation by using Incremental-Conductance Algorithm , with flow rate control. The Inc algorithm is optimized to operate under any insolation level throughout the operating region.

Predictive Control FS-MPC (torque and flux stator are controlled).

The high gain observer interconnected for sensor-less speed estimation of IM-Pump has been proposed here.

## 2 System architecture

Fig. 1 exhibits a simplified schema of a single stage solar PV array operated FS-MPC control of an IM motor for water pumping with maximum power point tracking algorithm and interconnected HO observe. This proposed system explains three-phase induction motor drive operated pump. The motor speed is estimated with one current sensor and one voltage sensor .Three-phase VSI switching is controlled by Finite-States Model Predictive Control. An incremental conductance (InC) algorithm is exercised for MPPT. The performance of gross system is display in subsequent sections under various conditions.

### 2.1 Design of Solar PV Array

The rating of motor induction is selected less than the PV array rating consequently the performance of this motor unaffected by the losses located in the inverter and motor .

For this work, a 3.7 kW PV array is constructed for system operation consisting of IMD of 3.5 kW. The equipment of PV array consists of 12 modules in parallel and 30 PV modules in series for short circuit current equal to 7.68 A and open circuit voltage equals 650V , respectively.

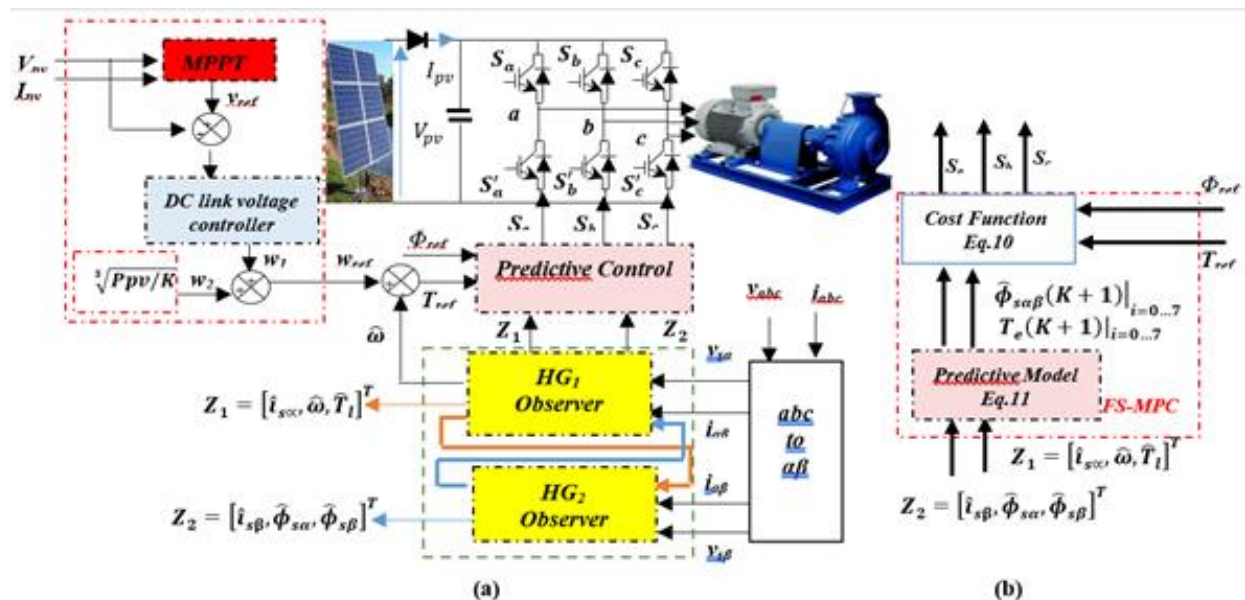


Fig. 1 Schematic diagram of Single Stage Solar Powered IM Drive. (a): all system bloc. (b): FS-MPC bloc

**Table 1 Specifications of pv array**

Voltage at Maximum MPP, $V_{mp}$	537V
Power at MPP, $P_{mp}$	3700W
Current at MPP, $I_{mp} = P_{mp}/V_{mp}$	7.63A
Number of module in series, $N_{ser} = V_{mp}/V_{mpp}$	30
Number of module in parallel, $N_{par} = I_{mp}/I_{mpp}$	12

**Table2 specifications of pv module**

Open Circuit Voltage $V_{oc}$ of one module	21.6V
Short Circuit Current $I_{sc}$ of one module	0.64A
Voltage at Maximum MPP, $V_{mpp}$	$0.81 * 21.6 = 17.6V$
Current at Maximum MPP, $I_{mpp}$	$0.9 * 0.64 = 0.58A$

## 2.2 Determination of DC-Link Voltage

The one of conditions about the control of inverter converter (output current) is the amplitude of input voltage should be high value than the value of line voltage specific to the motor [3]. The value of DC-Link voltage is given as:

$$V_{dc} > \sqrt{2} * V_l = \sqrt{2} * 380 = 537 V \quad (1)$$

Hence, the dc-link capacitor is given as per the equation is obtained in [17]. Therefore, the value is selected nearly 2500  $\mu F$ .

### 2.3 Selection of Water Pump

With water pumps, the relation between motor speed and load torque is relationship non-linear [1].

Therefore, the torque  $T_l$  is in proportion ( $K_{pm}$  : proportionality constant) to the square of the rated speed.

$$T_l = K_{pm} \omega_m^2 \quad (2)$$

### 3 Inc algorithm with flow rate control

The control of global system for Single Stage PV with IMD is comprised two parts, first one is the MPPT control to extract high power. It is achieved by three-phase inverter. The second one by using predictive controlled induction motor drive. The details are given in the following.

Fig. 1 shows the schematics of the technique MPPT for controlling the PV array voltage. The diverse MPPT techniques have been applied to track top power point, because there is a nonlinear relationship between voltage and power in solar PV array characteristic (fig.2).

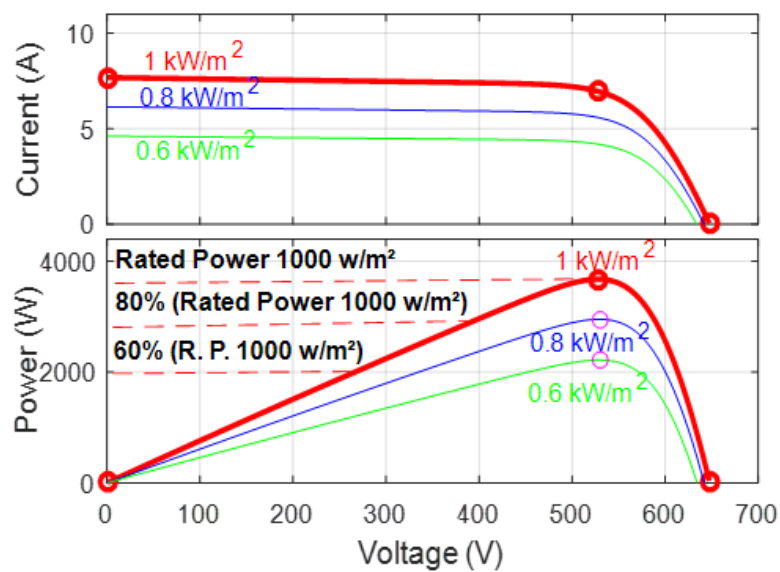


Fig 2 Ppv-Vpv curve for PV array

Figure 3 displays the basic scheme of the InC algorithm modified with the flow-rate power control. The idea came from the point of view of domestic water consumption . Where consumers can request smaller amounts of water drainage despite having a full insolation level [18].

According to the famous InC algorithm, it can be modified to some extent by operating the PV array at various operating point (10%, 20%,...100%) of rate power (1000 w/m2), as shown in Fig. 2, which corresponds to the desired flow rate at rated insolation.

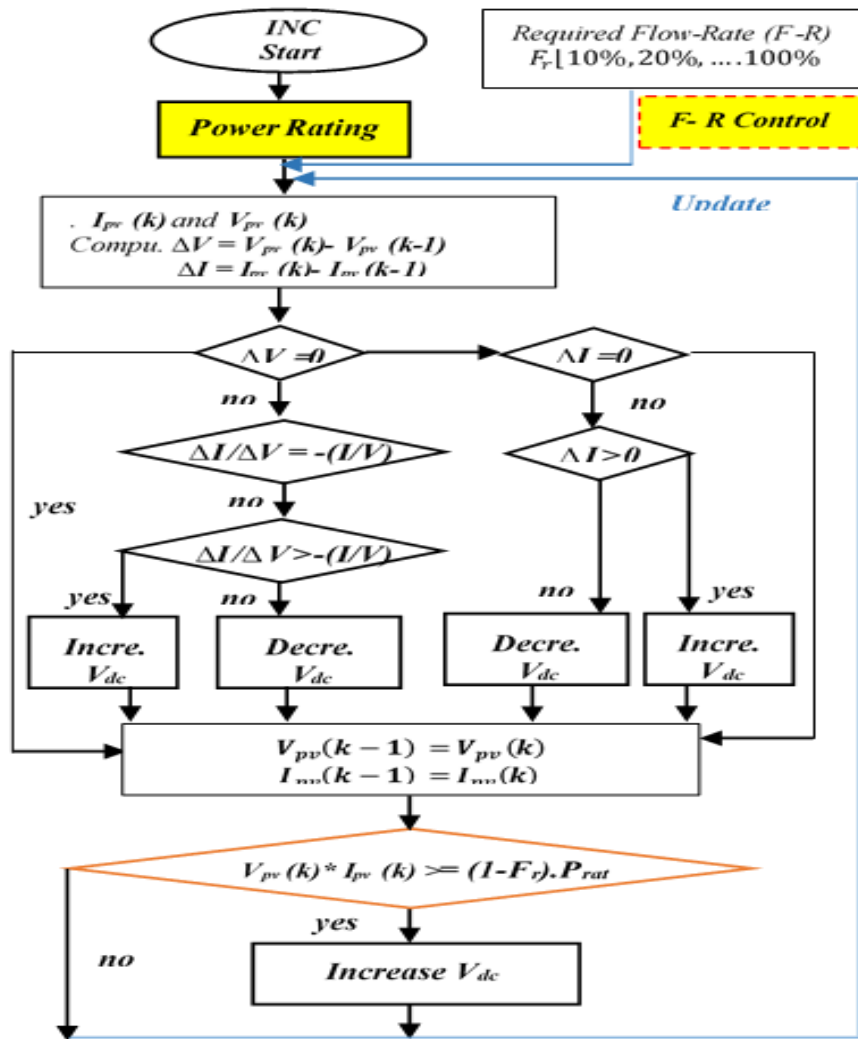


Fig.3 InC. Control Algorithm with flow rate control

Now, the reference speed can be achieved from the sum of two speeds. The first speed is obtained by comparing the voltage  $V_{pv}$  with the DC-link voltage  $V_{dc}^*$  (output of MPPT algorithm), which is fed to PI controller in order to get the speed ( $w_1$ ) and is given as follows,

$$\varepsilon_{vdc}(k) = V_{dc}^*(k) - V_{PV}(k) \quad (3)$$

$$w_1(k) = w_1(k-1) + K_{Pdc}(\varepsilon_{vdc}(k) - \varepsilon_{vdc}(k-1)) + K_{Idc}\varepsilon_{vdc}(k) \quad (4)$$

We can get the desired level reference velocity ( $\omega_{ref}$ ) from the PI controller. However, the dynamic response of the system in this case is very weak. For fast dynamic response, another speed is used with  $w_1$  (by instantaneous reflection of the PV energy on the motor speed). To derive the second speed  $w_{PV}$ , we use the pump convergence law by the following formula [9]:

$$w_{PV}(k) = \left( \frac{P_{PV}(k)}{K_{pm}} \right)^{1/3} \quad (5)$$

where  $K_{pm}$  is the proportionality constant.

From (4) and (5), we write the reference speed as :

$$w_{ref}(k) = w_1(k) + w_{PV}(k) \quad (6)$$

#### 4 Motor model

Induction motors drive are applied in the photovoltaic water pumping system because the performance and maintenance, as they are considered a reliable alternative The mathematical model of the motor is given in the frame of reference ( $\alpha$ - $\beta$ ), we added the load torque as another variable with the well-known state variables (constant currents and rotor flow, and angular velocity).

The load torque is known in our work through equation (2), the full model can be described by (1):

$$\begin{pmatrix} \dot{i}_{s\alpha} \\ \dot{i}_{s\beta} \\ \dot{\phi}_{r\alpha} \\ \dot{\phi}_{r\beta} \\ \dot{\Omega} \\ \dot{T}_L \end{pmatrix} = \begin{pmatrix} -F_1 i_{r\alpha} - F_2 \phi_{r\alpha} + F_3 \Omega \phi_{r\beta} \\ -F_1 i_{r\beta} - F_3 \Omega \phi_{r\alpha} + F_2 \phi_{r\beta} \\ F_4 i_{r\alpha} - F_5 \phi_{r\alpha} - p \Omega \phi_{r\beta} \\ F_4 i_{r\beta} + p \Omega \phi_{r\alpha} - F_5 \phi_{r\beta} \\ F_6 (\phi_{r\alpha} i_{r\beta} - \phi_{r\beta} i_{r\alpha}) - F_7 \Omega - F_8 T_L \\ 2F_9 \Omega \end{pmatrix} + \begin{pmatrix} F_{10} & 0 \\ 0 & F_{10} \\ 0 & 0 \\ 0 & 0 \\ 0 & 0 \\ 0 & 0 \end{pmatrix} \begin{pmatrix} u_{s\alpha} \\ u_{s\beta} \end{pmatrix}$$

The parameters  $F_{1,2,\dots,9}$  are defined as  $F_1 = \frac{1}{\sigma L_s} \left( R_s + \frac{L_m^2}{T_r L_r} \right)$ ,  $F_2 = \frac{1}{\sigma L_s} \left( \frac{L_m}{T_r L_r} \right)$ ,  $F_3 = \frac{p}{\sigma L_s} \left( \frac{L_m}{L_r} \right)$ ,  $F_4 = \left( \frac{L_m}{T_r} \right)$ ,  $F_5 = \left( \frac{1}{T_r} \right)$ ,  $F_6 = \left( \frac{p L_m}{J L_r} \right)$ ,  $F_7 = \left( \frac{f_v}{J} \right)$ ,  $F_8 = \left( \frac{1}{J} \right)$ ,  $F_9 = K_{PV}$ ,  $F_{10} = \frac{1}{\sigma L_s}$ .

Where:  $\sigma = 1 - \left( \frac{L_m^2}{L_s L_r} \right)$ ,  $T_r = \left( \frac{L_r}{R_r} \right)$ ,

On the other hand, the parameters ( $R_r$ ,  $R_s$ ) are respectively rotor and stator resistance ,for the inductances ( $L_r$ ,  $L_s$ ,  $L_m$ ) are respectively stator, rotor and mutual inductances, finally  $p$  is the number of pair poles.

#### 5 Predictive FS-MPC control

From Fig. 1(b), it can be seen the conventional predictive control FS-MPC where the cost function is the criterion for selecting the optimal voltage vector among the eight feasible ones with a traditional 2-level VSI inverter.

The switching states  $S$  and the output voltage  $V_S$  can be expressed as:

$$S = \frac{3}{2} (S_a + e^{j2\pi/3} S_b + e^{j4\pi/3} S_c) \quad (8)$$

$$V_s(S_{a,b,c}) = \sqrt{\frac{2}{3}} \frac{V_{dc}}{2} (S_a + e^{j2\pi/3} S_b + e^{j4\pi/3} S_c) \quad (9)$$

On the other hand, the torque and stator flux are directly controlled using the cost function [10], and the expected values of these items in (10) with their references are used to reduce the absolute error, and after that the optimal voltage vector is selected.

$$F_{|i=1:8} = abs\left(T_e^* - T_e^p(k+1)\right) - \gamma_\psi * abs\left(\Phi_s^* - \Phi_s^p(k+1)\right) \quad (10)$$

Where  $\gamma_\psi$  is the weighting factor which denotes the balance between all terms in cost function ,but finding this value is very time consuming and tedious.

Here, using the model (7) and the forward Euler approximation (discrete model) [ 19], we can get the predicted values of stator flux and torque (predictive model) :

$$\begin{aligned} \phi_s(k+1) &= \phi_s(k) + T_s V_s(k+1) - R_s I_s(k) \\ i_s(k+1) &= \left(1 - \frac{T_s R_\tau}{L_s \sigma}\right) i_s(k) + ((\tau_r k_r - j k_r w_m) \phi_s(k) + V_s(k+1)) \end{aligned}$$

$$T_e(k+1) = \frac{3}{2} p \phi_s(k+1) \cdot i_s(k+1) \quad (11)$$

From equation (10), and (11), using the conventional FS-MPC, it can be seen that finding the output voltage vector (the optimal vector) for a two-level inverter requires 8 torque predictions, 8 stator flux predictions, and 8 cost function evaluations. Which takes a lot of time [13,14].

## 6 Interconnected high-gain observe

With nonlinear system of induction motor model, it is difficult to find a regular method to design an observer for the full system [20]. To solve this problem we propose an interconnected observer or between two subsystems of the full model for the motor-pump . It is satisfies some required properties. Hence, the states of each of the two systems are available for the other system. With this aim, the model of induction motor (7) can be rewritten into two interconnected systems:

$$\begin{bmatrix} \dot{i}_{s\alpha} \\ \dot{\Omega} \\ \dot{T}_l \end{bmatrix} = \begin{bmatrix} 0 & F_3 \phi_{r\beta} & 0 \\ 0 & 0 & -F_8 \\ 0 & 0 & 0 \end{bmatrix} \begin{bmatrix} i_{s\alpha} \\ \Omega \\ T_l \end{bmatrix} + \begin{bmatrix} -F_1 i_{s\alpha} + F_2 \phi_{r\alpha} + F_{10} u_{s\alpha} \\ F_6 (\phi_{r\alpha} i_{s\beta} - \phi_{r\beta} i_{s\alpha}) - F_7 \Omega \\ 2F_9 \Omega \end{bmatrix} \quad (12)$$

$$\begin{bmatrix} \dot{i}_{s\beta} \\ \dot{\phi}_{r\alpha} \\ \dot{\phi}_{r\beta} \end{bmatrix} = \begin{bmatrix} -F_1 & 0 & F_2 \\ 0 & -F_5 & 0 \\ -F_2 & 0 & -F_5 \end{bmatrix} \begin{bmatrix} i_{s\beta} \\ \phi_{r\alpha} \\ \phi_{r\beta} \end{bmatrix} + \begin{bmatrix} -F_3 \Omega + F_{10} u_{s\beta} \\ -p\Omega + F_4 i_{s\alpha} \\ -p\Omega \phi_{r\alpha} + (F_2 + F_4) i_{s\beta} \end{bmatrix} \quad (13)$$

The torque  $T_l$  represents the load torque of the water pumps, which is proportional to the square of the rated speed as (4). On other hand, the variables current and voltage of motor-pump system are measured.

The variables of two subsystem has been considered in order to separate in one subsystem the magnetic variables and in the other one the mechanical variables.



$$\begin{aligned} \dot{X}_1 &= A_{hg1}(u, y, X_2)X_1 + g_{hg1}(u, y, X_2, X_1) \\ y_1 &= C_1X_1 \end{aligned} \quad (14)$$

$$\begin{aligned} \dot{X}_2 &= A_{hg2}X_2 + g_{hg2}(u, y, X_2, X_1) \\ y_2 &= C_2X_2 \end{aligned} \quad (15)$$

Where  $u = [u_{s\alpha} u_{s\beta}]'$  can be an input,  $\tilde{X}_1 = [i_{s\alpha} \quad \Omega \quad T_{l1}]'$ ,  $X_2 = [i_{s\beta} \quad \phi_{r\alpha} \quad \phi_{r\beta}]'$ ,  $y = [i_{s\alpha} i_{s\beta}]'$ ,  $C_1 = C_2 = [1 \quad 0 \quad 0]'$ .

$$A_{hg1}(u, y, X_2) = \begin{bmatrix} 0 & F_3\phi_{r\beta} & 0 \\ 0 & 0 & -F_8 \\ 0 & 0 & 0 \end{bmatrix}$$

$$g_{hg1}(u, y, X_2, X_1) = \begin{bmatrix} -F_1i_{s\alpha} + F_2\phi_{r\alpha} + F_{10}u_{s\alpha} \\ F_6(\phi_{r\alpha}i_{s\beta} - \phi_{r\beta}i_{s\alpha}) - F_7\Omega \\ 2F_9\Omega \end{bmatrix}$$

$$A_{hg2} = \begin{bmatrix} -F_1 & 0 & F_2 \\ 0 & -F_5 & -1/j \\ -F_2 & 0 & -F_5 \end{bmatrix}$$

$$g_{hg2}(v, X_1, X_2) = \begin{bmatrix} -F_3\Omega + F_{10}u_{s\alpha} \\ -p\Omega + F_4i_{s\alpha} \\ -p\Omega\phi_{r\alpha} + (F_2 + F_4)i_{s\beta} \end{bmatrix}$$

Objective: Our main objective is to design an Interconnected high-gain observer for subsystems (12) and (13) by Using currents and voltages as measured values for an induction motor- pump water.

The first observer in Fig. 1 allows to observe the speed and load torque of motor-pump while the second is consecrated to estimate the stator fluxes.

In order to design two interconnected observers for (12) and (13) and with some assumption [15], the high-gain observer for subsystem (14) and (15) are given by:

$$\begin{cases} \dot{Z}_1 = A_{hg1}(u, y, Z_2)Z_1 + g_{hg1}(u, y, Z_2, Z_1) + S_1^{-1}C_1^T(y_1 - \hat{y}_1) \\ \dot{S}_1 = -\theta_1S_1 - A_{hg1}^T(u, y, Z_2)S_1 - S_1A_{hg1}(v, Z_2) + C_1^TC_1 \\ \hat{y}_1 = C_1Z_1 \end{cases} \quad (16)$$

$$\begin{cases} \dot{Z}_2 = A_{hg2}Z_2 + g_{hg2}(u, y, Z_2, Z_1) + S_2^{-1}C_2^T(y_2 - \hat{y}_2) \\ \dot{S}_2 = -\theta_2S_2 - A_{hg2}^T(u, y, Z_2)S_2 - S_2A_{hg2} + C_2^TC_2 \\ \hat{y}_2 = C_2Z_2 \end{cases} \quad (17)$$

Note that:  $S_1^{-1}C_1^T$  and  $S_2^{-1}C_2^T$  are the gains of our observers

Where:  $Z_1 = [\hat{i}_{s\alpha} \quad \hat{\Omega} \quad \hat{T}_l]'$ ,  $Z_2 = [\hat{i}_{s\beta} \quad \hat{\phi}_{r\alpha} \quad \hat{\phi}_{r\beta}]'$ ,  $C_1 = C_2 = [1 \quad 0 \quad 0]'$ .  $u = [u_{r\alpha} u_{s\beta}]'$  is the input of the high-gain observer and  $y = [i_{s\alpha} i_{s\beta}]'$  is the output.

Remark1. In order to ensure the convergence of this observer, sufficient conditions are established where the values of  $\theta_1$  and  $\theta_2$  are positive and large enough [20-15].

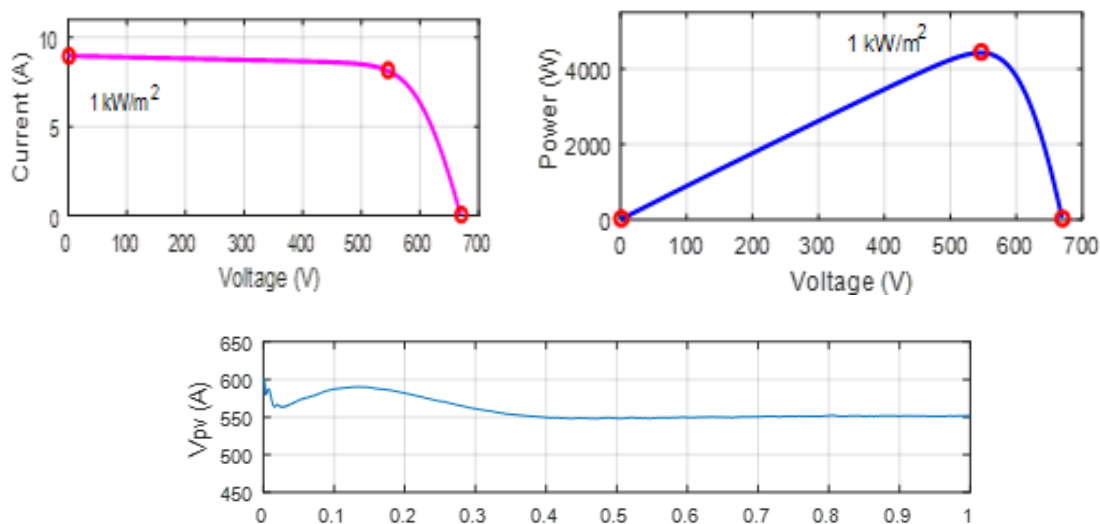
Remark2. When the induction motor is under or near unobservable conditions, we modify the second observer to an estimator (without error gains) see [16]. In this work, the reference value of speed is a function of irradiation and therefore, the pump load changes and hence varying the phase current of the motor [6]. Thus, the induction motor operates at a high or medium speed under observable conditions then the proposed observer operates as an observer.

## 7 Simulation results

This section treats with performance of the single stage solar PV system subjected to various atmospheric conditions, The pump load ( $T_p$ ) is automatically varied as the insolation is changed. The details are given in the following.

### 7.1 Performance of the system at Starting state

From Fig. 4, The system is initially tested directly at  $1000 \text{ W/m}^2$ . When the system is running, MPPT is quickly reached. Where the figure shows an increase of photovoltaic power ( $P_{pv}$ ) and PV voltage ( $V_{pv}$ ), which stabilizes this values ( $V_{pv}$ ,  $I_{pv}$  and  $P_{pv}$ ) at maximum MPP point within fraction of second (about 0.2s).



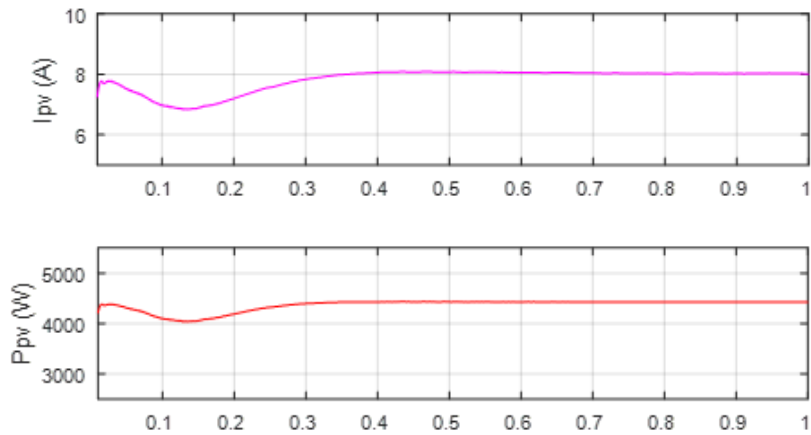


Fig. 4 Starting and steady-state performance of PV array

### 7.2 Dynamic Performance of Proposed Control

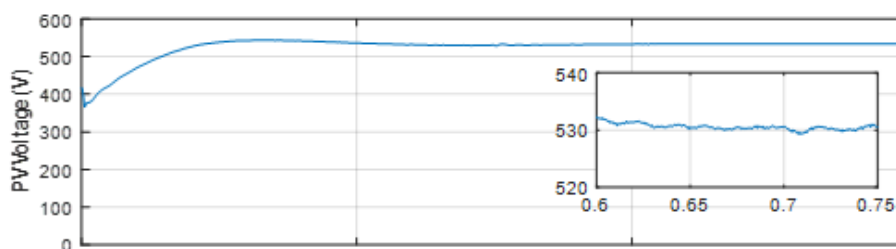
Fig.5 (a,b) display the favorable dynamic and steady performance of the all system (PV system with motor-pump) of predictive control (FS-MPC) when insolation level is reduced from 1000W/m<sup>2</sup> to 700W/m<sup>2</sup> after 0.75s.

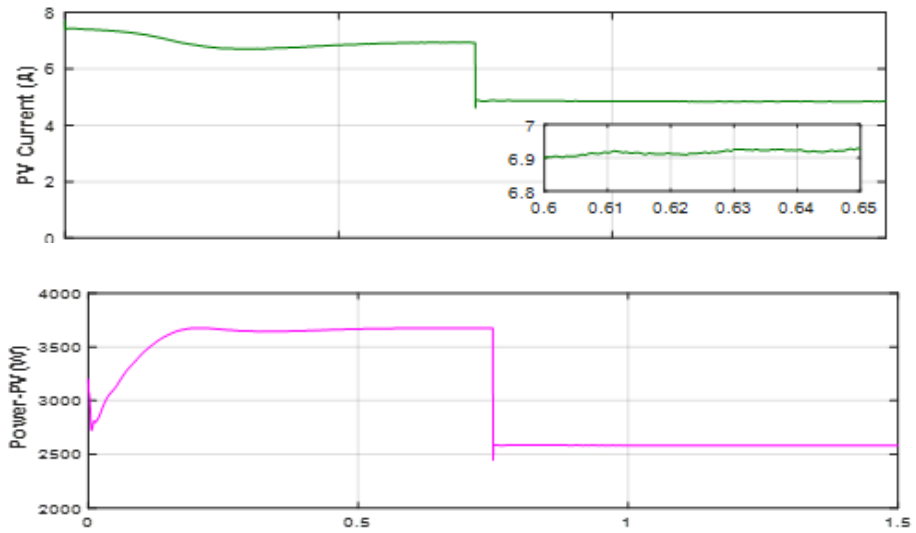
Firstly, from the fig. 5(a) , there is slight change in the voltage  $V_{pv}$  at maximum power however, the current  $I_{pv}$  at MPP change significantly, this change have been shown in Figs. 3 for the PV array characteristics . Once MPP is tracked, the technique MPPT (InC) for controlling the  $V_{pv}$  maintains it at the same point.

Rated-speed transient behavior of the proposed FS-MPC control is presented in Fig. 5 during step change in insolation (1000 W/m<sup>2</sup> to 700 W/m<sup>2</sup>). The curves are arranged from top to bottom, the curves are the reference speed and estimated speed, load torque and estimated torque, stator current, stator flux and stator voltage.

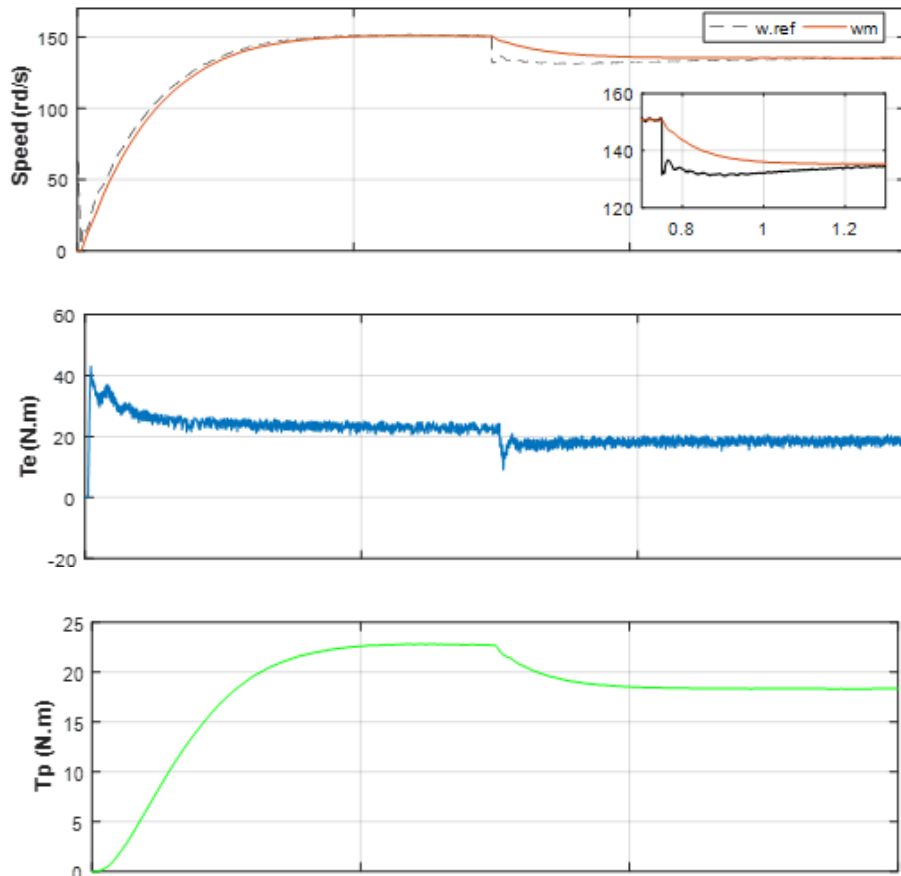
It is clear from the waveforms that the system behaves satisfactorily as the insolation is changed at 0.75 s. The reference speed depends on insolation.

When there is change in insolation, the MPP is moved to new operating point (700 w/m<sup>2</sup>). This leads to a new reference speed of approximately 135 (rad/s).the motor speed with the proposed control can track the reference speed accurately with quickly response.





(a)



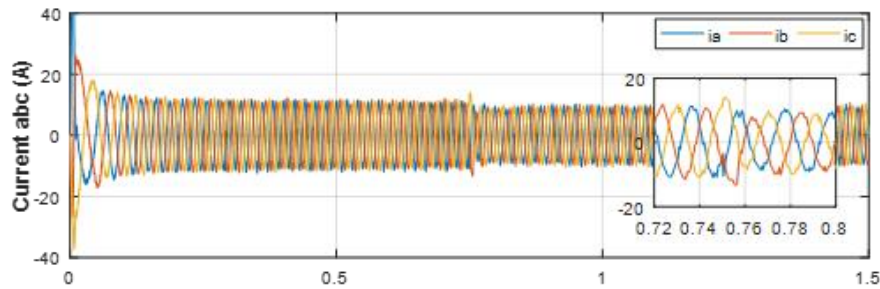


Fig.5 Dynamic of the system when insolation level is reduced from 1000 to 700W/m<sup>2</sup> with FS-MPC.(a)PV array. (b) IMD

At 0.75 s, the change of speed is followed by the change of the corresponding load torque  $T_p$  (pump torque), as described in (2). Thus changing the phase current of the motor and variation of the electromagnetic torque  $T_e$ , which settles at a new level corresponding to the new pump torque, as can be seen in all curves.

### 7.3Performances of the HG -Interconnected

The proposed interconnected high gain observers is tested at low insolation where the reference speed is calculated by adding speed derived from the voltage controller output and from PV power.

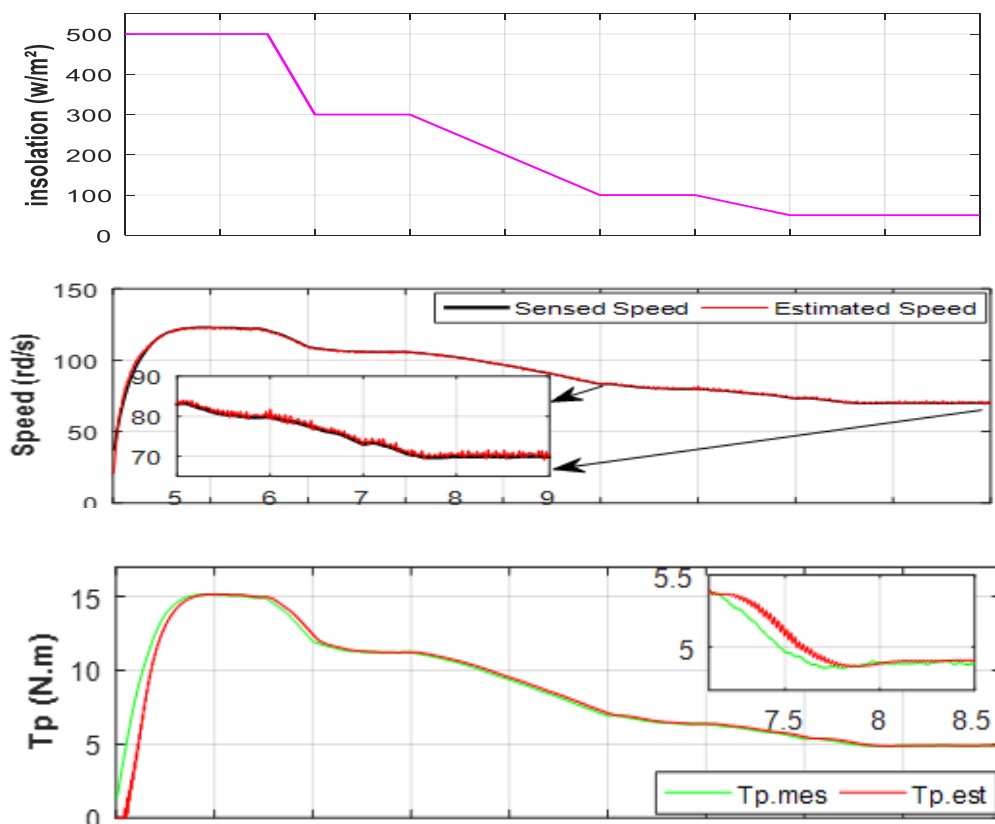


Fig.6 Performances of HG -Interconnected when insolation level is reduced from 500 to 50W/m<sup>2</sup>

Fig. 6 show the two speed  $\omega_{sen}$  and  $\omega_m$  during dynamic and steady condition when insolation level is reduced from 500 to 50W/m<sup>2</sup>. It is observed from these results that estimated speed ( $\omega_m$ ) precisely follows sensed speed ( $\omega_{sen}$ ) and the error speed signal is nearly zero in steady state condition. The same analysis and conclusions are given for pump torque.

The isolation level is changed from 1000 W/m<sup>2</sup> to 800,600 and 500 W/m<sup>2</sup>, which leads to a new reference speed. According to the results, quick response of motor speed, in addition to the accurate tracking of the reference speed. On the other hand, the change in speed corresponds to a change in the load torque  $T_p$  (pump torque), as described in (2). Thus changing the phase current of the motor and the variation of the electromagnetic torque  $T_e$ . Table 4 and Fig. 7 summarize the performance of the system at each insolation level.

Table 4. Performance of the system at different insolation

<i>Insolation</i> (W/m <sup>2</sup> )	$P_{pv}$ (W)	$V_{pv}$ (V)	$I_{pv}$ (A)	$\omega_m$ (rd/s)	$T_p$ (N.m)
1000	3700	536	7	152	24
800	2955	536	5.7	140	20
600	2204	535.5	4.1	134	17
500	1910	535	3.6	128	15

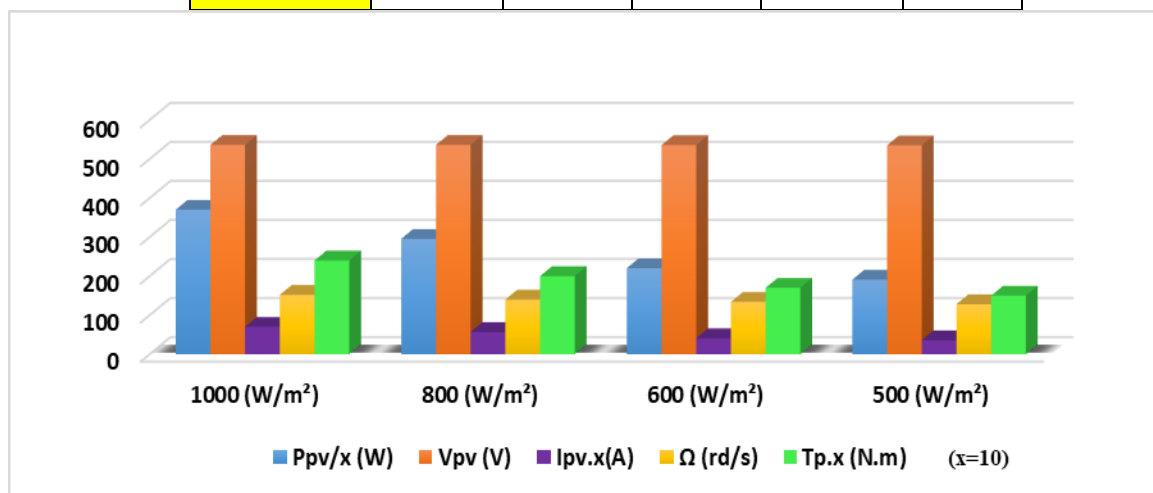


Fig. 7. Graphical variation curve of the system at different insolation

## 8. Conclusion

In this work, the proposed single stage solar PV array fed water pumping system has been simulated, we examined in this system three predictive technics applied to a two-level inverter. Some conclusions can be written as follows:

- 1)The results showed better performance and more stability under steady state and dynamic conditions with FS-MPC technique
- 2)The results of the improved MPPT technology have displayed a suitable solution to control of the flow according to the requirements of the consumer.
- 3)The proposed interconnected observer of the sensor-less motor-pump were used to achieve an exponential speed and flux tracking for induction motor without measurements of rotor speed and load torque. at low insolation, the results have showed estimated motor speed converges to the measured speed.

## Appendices

### - Solar PV Array (Simulation Data)

$V_{oc}=760V$ ,  $V_{mp}=600 V$ ,  $I_{sc}=16 A$ ,  $I_{mpp}=14.5 A$ ,  $N_{ser}=34$ ,  $N_{par}=12$ ,  $(f_s)= 10 kHz$ , DC-link Capacitor ( $C_{dc}$ )= 2500  $\mu F$ .

### - Induction Motor Parameters (Simulation Data)

3.5 kW, 3-phase, 380 V (L-L), 4 poles,  $R_s=0.7384 \Omega$ ,  $R_r= 0.7043 \Omega$ ,  $L_s= 0.003045 H$ ,  $L_r= 0.003045 H$ ,  $L_m=0.1241 H$ ,  $J=0.0343 Kg\cdot m^2$ .

## References

- [1] S. Shukla and B.Singh, "Single-Stage PV-Grid Interactive Induction Motor Drive with Improved Flux Estimation Technique for Water Pumping with Reduced Sensors". DOI 10.1109/TPEL.2020.2990833, IEEE Transactions on Power Electronics 2020.<https://ieeexplore.ieee.org/document/9082185>
- [2] S. Shukla and B.Singh, "Reduced Sensor Based PV Array Fed Direct Torque Control Induction Motor Drive for Water Pumping". DOI 10.1109/TPEL.2018.2868509, IEEE Transactions on Power Electronics 2018.<https://ieeexplore.ieee.org/document/8454312>
- [3] S. Shukla and B. Singh, "Single Stage PV Array Fed Speed Sensorless Vector Control of Induction Motor Drive for Water Pumping". DOI 10.1109/TIA.2018.2810263, IEEE Transactions on Industry Applications 2018.<https://ieeexplore.ieee.org/document/8304696>
- [4] S. Shukla and B. Singh, "Single-Stage PV-Grid Interactive Induction Motor Drive with Improved Flux Estimation Technique for Water Pumping with Reduced Sensors". DOI 10.1109/TPEL.2020.2990833. IEEE Transactions on Power Electronics 2020.<https://ieeexplore.ieee.org/document/9082185>
- [5] S. Shukla and B. Singh, "Reduced Current Sensor Based Solar PV Fed Motion Sensorless Induction Motor Drive for Water Pumping .IEEE transactions on industrial informatics, vol. 15, no. 7, july 2019.<https://ieeexplore.ieee.org/document/8570765>

- [6] K. Khan, S. Shukla and B. Singh, "Improved Performance Design Realization of Fractional kW Induction Motor with Predictive Current Control for Water Pumping". DOI 10.1109/TIA.2020.2968014, IEEE Transactions on Industry Applications. <https://ieeexplore.ieee.org/document/8963667>
- [7] M. Lv , S. Gao, Y. Wei , D. Zhang , H. Qi and Y. Wei, "Model-Free Parallel Predictive Torque Control Based on Ultra-Local Model of Permanent Magnet Synchronous Machine," *Actuators* 2022, 11, 31. <https://doi.org/10.3390/act11020031>
- [8] Y. Wang, L. Zhou, S. A. Bortoff, A. Satake, and S. Furutani, "High gain observer for speed-sensorless motor drives: Algorithm and experiments," in 2016 IEEE International Conference on Advanced Intelligent Mechatronics (AIM), 2016, pp. 1127-1132. <https://ieeexplore.ieee.org/document/7576921>
- [9] C. Wang , D. Cao , X. Qu and C. Fan," An Improved Finite Control Set Model Predictive Current Control for a Two-Phase Hybrid Stepper Motor Fed by a Three-Phase VSI ", *Energies* 2022, 15, 1222. <https://doi.org/10.3390/en15031222>
- [10] Z. Lammouchi , K. Barra , " Particle swarm weighting factor optimization for predictive control of three level inverter with balanced voltages" . *Int. J. Power Electronics*, Vol. 12, No. 3, 2020. <https://www.inderscience.com/info/inarticle.php?artid=110064>
- [11] Z. Lammouchi , Y. Bekakra," Predictive Direct Power Control for photovoltaic Grid Connected System with Reduction of Switching Frequency", 1st International Conference on Communications, Control Systems and Signal Processing (CCSSP). IEEE, N 19867531, 16-17 May 2020. <https://ieeexplore.ieee.org/document/9151724>
- [12] F. Sebaaly, Mo. Sharifzadeh, , Y. Kanaan, and K. Al-Haddad, " Mode Operation of Finite Set Model Predictive Control for Grid-Connected Packed E-Cell (PEC) Inverter," *IEEE Transactions on Industrial Electronics*, June 28, 2020. <https://ieeexplore.ieee.org/document/9126237>
- [13] T. Orłowska-Kowalska, M. Korzonek, and G. Tarchala, "Double Vectors Model Predictive Torque Control Without Weighting Factor Based on Voltage Tracking Error". *IEEE TRANSACTIONS ON POWER ELECTRONICS*, VOL. 33, NO. 3, MARCH 2018. <https://ieeexplore.ieee.org/document/7893710>
- [14] N. Bekhoucha, , M. Kermadi, N. Mesbahi, and S. Mekhilef, "Performance Investigation of Deadbeat Predictive Controllers for Three-Level Neutral Point Clamped Inverter " . *IEEE Journal of Emerging and Selected Topics in Power Electronics*. .DO.10.1109/JESTPE.2021.3092057. <https://ieeexplore.ieee.org/document/9464350>
- [15] M. Ghanes, J. De Leon and A. Glumineau., "Observability Study and Observer-Based Interconnected Form for Sensorless Induction Motor," *IEEE Conference on Decision & Control*; Manchester Grand Hyatt Hotel San Diego, CA, USA, December 13-15, 2006 . <https://ieeexplore.ieee.org/document/4177591>
- [16] D. Traoré , J. De Leonb, A. Glumineaua, "Adaptive interconnected observer-based backstepping control design for sensorless induction motor"



doi:10.1016/j.automtica.2012.01.018.<https://dl.acm.org/doi/abs/10.1016/j.automtica.2012.01.018>

- [17] K. Khan, S. Shukla and B. Singh, "Performance-Based Design of Induction Motor Drive for Single-Stage PV Array Fed Water Pumping". IEEE Trans. Ind. Applications , Vol. 55, NO. 4, JULY/AUGUST 2019.<https://ieeexplore.ieee.org/document/8686120>
- [18] O. Sandre, S. Jorge ,C.-Rojas, Jesus P. Ordaz and C. Cuvas, "Stator Fixed Deadbeat Predictive Torque and Flux Control of a PMSM Drive with Modulated Duty Cycle," Energies 2021, 14, 2769. <https://doi.org/10.3390/en14102769>.
- [19] M.Lv , S. Gao , Y.Wei , D. Zhang \* , H. Qi and Y. We "Model-Free Parallel Predictive Torque Control Based on Ultra-Local Model of Permanent Magnet Synchronous Machine" Actuators 2022, 11, 31. <https://doi.org/10.3390/act11020031>.
- [20] Naifar, O., et al., A comparative study between a high-gain interconnected observer and an adaptive observer applied to IM-based WECS. The European Physical Journal Plus, 2015. 130: p. 1-13.<https://doi.org/10.1140/epjp/i2015-15088-2>